

THE ORIGINAL METHOD FOR ASSESSMENT OF RESIDUAL STRESSES IN REINFORCED SURFACE LAYERS

KIANICOVÁ Marta¹, POKLUDA Jaroslav^{1,2}, HORNÍKOVÁ Jana², ŠANDERA Pavel²

¹Alexander Dubček University of Trenčín, Trenčín, Slovakia, EU

²Brno University of Technology, Brno, Czech Republic, EU

Abstract

An original method was recently developed for an assessment of residual stresses in case-hardened steels based on S-N curves of hardened and virgin samples along with the measurement of location of fish-eye crack centres. This method is applicable only when the surface of virgin specimens is sufficiently smooth to avoid the initiation of fatigue cracks from large surface defects. A systematic study focused on identification of the applicability range was started using specimens with extremely rough surfaces finished by turning. The analysis yielded compressive stresses up to 700 MPa at the hardened surface and high tensile stresses up to 500 MPa in the specimen bulk. The most probable location of fish-eye centres was, however, predicted to be in a significantly higher depth than that found in the real specimens. This could be attributed to the large surface damage induced by turning which, therefore, lies beyond the acceptable range of surface machining.

Keywords: Nitrided steel, residual stress, fish-eye crack, S-N curves

1. INTRODUCTION

The coated materials rapidly become an increasing importance for many engineering components since they improve the structural integrity in various aspects. With respect to their function, the coatings can be divided into two main classes: (i) surface protection and (ii) surface hardening [1]. Diffusion aluminide coatings (DACs), overlay coatings (OLCs) and thermal barrier coatings (TBCs) are typical representatives of the first class. The most popular representatives of the second class are carburized, nitrided or carbonitrided surface layers (CNSLs) produced by diffusion processes. They increase the surface hardness of a substrate material and introduce compressive residual stresses [2, 3].

The recent knowledge of crack initiation and propagation mechanisms in materials with CNSL is rather good. It is well known that a higher strength of CNSLs and a presence of compressive residual stresses are the main reasons for improved fatigue strength. Since such layers hinder the dislocation motion, the predominant failure mechanism in the high cycle fatigue region is the subsurface fatigue crack growth [4]. As a rule, the cracks initiate on the internal inclusions within the innermost sub-layer of the hardened surface layer and propagate in a near vacuum by forming so-called fish-eye cracks (see **Figures 1 and 2**). When the crack front approaches the low-toughness CNSL, a local through-the-layer brittle cracking creates a connection to the surface and, subsequently, a penetration of the atmosphere inside the fish-eye. This changes the growth mechanism to an environmentally assisted one which leads to a different surface roughness and the optical contrast. The fish-eye cracks are usually of either a circular or an elliptical shape depending on the type of loading (push-pull, rotating bending/plane bending) and the absence / presence of high compressive residual stresses introduced by some of the surface hardening procedures [5].

It should be noted that the fish-eye cracks can also be found on fracture surfaces of uncoated metallic materials loaded in the ultra-high cycle fatigue region. It was theoretically predicted and experimentally confirmed that, in this case, the crack initiation stage covers more than 95 % of fatigue life (e.g., [6, 7]).

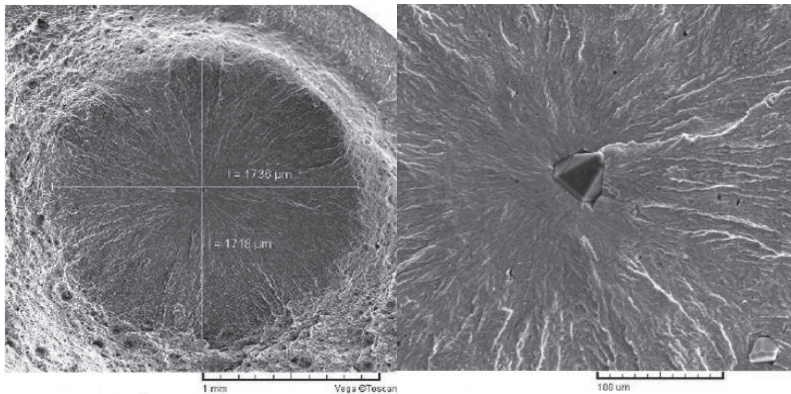


Figure 1 Fish-eye crack in a nitrided specimen; a) the global SEM view b) inclusion in the fish-eye centre.

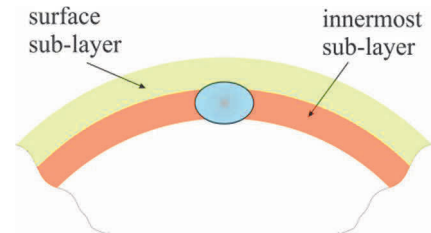


Figure 2 Scheme of CNTL sub-layers with a fish-eye crack on the fracture surface.

This article is devoted to an assessment of residual stresses in a nitrided high-strength steel using an original method recently published by the authors [5]. This simple method can be employed as an alternative measurement of residual stresses within hard surface layers that are usually performed by means of methods based on different physical principles as X-ray, magnetism or mechanical removal of material.

The new method is relevant only when the surface of virgin specimens is sufficiently smooth to avoid the initiation of fatigue cracks from large surface defects (artificial intrusions) made by machining. Therefore, the range of its applicability is limited by a still acceptable upper bound of surface roughness of virgin specimens, identification of which is the aim of recently started systematic investigation. This article reports on the first research result achieved by using samples with extremely rough surfaces.

2. BRIEF DESCRIPTION OF THE NEW METHOD

In the pure rotating bending, the direction of internal stresses is equal to that of the main stress. The orientation of the residual stress vector is opposite to that of the main stress during the tensile loading half cycle and identical during the compressive half cycle. This means that, in the bulk of the nitrided specimens, the presence of residual stresses σ_{res} shifts the S-N (Wöhler) curve for a symmetric loading ($R = -1$) of the virgin specimens to different curves corresponding to lower ($R < -1$) or higher ($R > -1$) cyclic ratios. To correctly assess the effect of residual stresses on this shift, therefore, the values of external (applied) stress at the initiation sites (centres of primary fish-eyes) must be precisely identified. The difference between this internal S-N curve and that for the virgin specimens (without the nitrided layer) is a measure of residual stress levels in the depths corresponding to crack initiation sites. Thus, the new method for residual stress assessment consists of several procedures applied to fracture surfaces and both above mentioned S-N curves as described below in a stepwise manner:

- (i) Measurement of the distance of the k -th fish-eye centre from the specimen surface in the radial direction. This distance is called an initiation depth h_k ;
- (ii) Calculation of the amplitude of the bending stress σ_{ak} that corresponded to the initiation depth h_k on the fracture surface of the k -th specimen during its rotating bending loading;
- (iii) Identification of the number of cycles to failure N_{fk} corresponding to the k -th specimen in the rotating bending test;
- (iv) Determination of the stress amplitude σ_{ak} on the surface of uncoated specimens that corresponded to the number of cycles to failure N_{fk} according to the Wohler curve for uncoated specimens;

- (v) Employment of both the ratio $\bar{\sigma}_{ak} / \sqrt{\sigma}_{ak}$ and the relationship generally describing the shift of S-N curves (according to Soderberg or Goodman approximations [5]) to determine the mean stress $\sigma_{mk} = \sigma_{res,k}$ corresponding to the depth h_k within the coating.

The construction of the shape of whole residual-stress surface related to the specimen cross-section from the fish-eye data, which are restricted just to the innermost sub-layer, is enabled by knowledge of some necessary physical rules and positions of special sets of points:

- (vi) The residual-stress profile possesses a characteristic, circularly symmetric shape that can be mathematically described by a multi-parameter function $\sigma_{res}(h) = A_1(\exp(-A_2(h + A_3)) - \exp(-A_4(h + A_3)))(h - A_5)$, where A_1, \dots, A_5 are fitting parameters.
- (vii) The value of the surface integral of residual stresses throughout the specimen cross-section must be zero.
- (viii) The positions of both the zero-stress (transition compressive-tensile) and the maximum tensile-stress circles on the cross-section are determined by the innermost data.

Figure 3 shows a comparison of the experimental stress profile determined by X-ray diffraction with that constructed from the fish-eye data obtained from nitrided samples made of high-strength steel [5]. The surface roughness of virgin samples corresponded to a standard grinding number of 0.32.

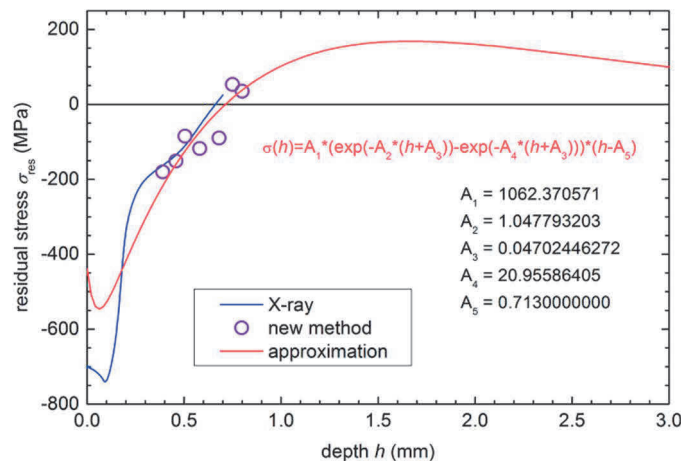


Figure 3 Stress profiles obtained by experiment (X-ray) and approximation of fish-eye data (new method) for nitrided specimens with surfaces finished by fine-grinding

3. EXPERIMENTAL MATERIAL AND S-N CURVES

The specimens were made of quenched and tempered 31CrMoV9 high-strength steel with surfaces hardened by diffusion nitriding. The chemical composition of this steel is in **Table 1** and the basic mechanical properties are shown in **Table 2**, the hardness value of HV 784 in 0.1 mm depth. The final machining of the specimens was made just by turning which left circumferential scratches on the surface even visible to the naked eye - see **Figure 4**. The S-N curves of nitrided and virgin specimens are plotted in **Figure 5** along with experimental data.

One can see that there is a significant scatter of the S-N data of virgin specimens especially in the high-cycle region and near the fatigue limit that is a consequence of their rough surfaces. In this region, the S-N curve of virgin specimens is significantly shifted down with respect to the S-N curve for nitride specimens. Thus, there is a large improvement of the fatigue limit due to the surface hardening and partial smoothing caused by the nitriding process. Indeed, the fatigue limit of virgin specimens is more than two times lower than that of the nitrided ones.



Figure 4 Circumferential micro-scratches on the specimen surface caused by turning

Table 1 Chemical composition of the 31CrMoV9 high-strength steel

C	Si	Mn	P	S	Cr	Ni	Mo	Al	Cu	Co
0.321	0.256	0.664	0.012	0.027	2.58	0.134	0.229	0.022	0.167	0.0068

Ti	Nb	V	W	Pb	B	Sb	Sn	Zn	As	Bi
0.0023	0.0038	0.184	0.007	0.0014	0.008	0.0027	0.01	0.004	0.0049	0.0015

Ta	Ca	Ce	Zr	La	Se	N	Fe	Cr+Mo+Ni
0.007	0.005	0.002	0.0015	0.0003	0.002	0.0085	95.36	2.94

Table 2 Mechanical properties of the 31CrMoV9 high-strength steel

Ultimate stress σ_u (MPa)	Yield stress σ_y (MPa)	Elongation (%)
1048	957	15

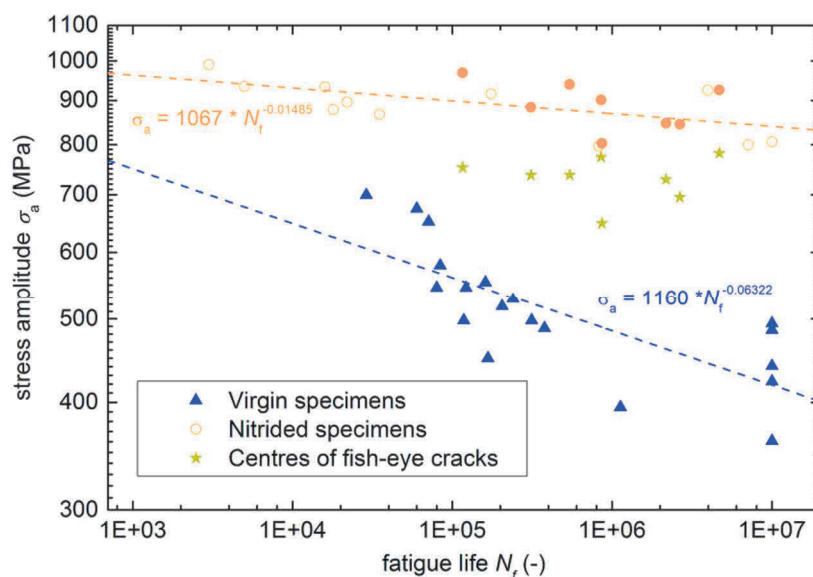


Figure 5 The S-N curves of nitrided and virgin specimens along with experimental data

4. EVALUATION OF RESIDUAL STRESSES

The data reflecting the amplitude of the bending stress σ_{ak} corresponding to the depth h_k of the k-th fish-eye centre on the fracture surface are plotted as solid circles in **Figure 5**. All these data lie in between the SN curves of virgin and nitrided specimens and, therefore, they all lie in the region of compressive residual stresses. The related values of residual stresses $\sigma_{res,k}$, computed using the Soderberg approximation, are plotted in dependence of the depth h_k in **Figure 6** along with the fitting curve $\sigma_{res}(h)$ determining the profile of calculated residual stresses inside the nitrided specimens.

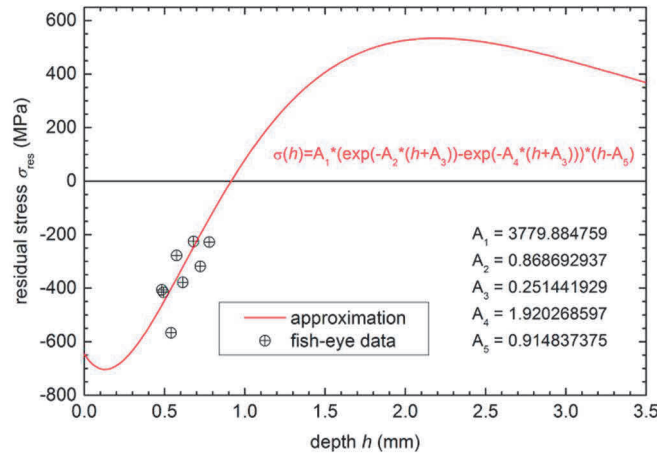


Figure 6 The fitting curve $\sigma_{res}(h)$ determining the profile of calculated residual stresses inside the nitrided specimens with surfaces finished by turning.

One can observe that the tensile values of the fitting curve $\sigma(h)$ deep in the specimen core are very high. This indicates that this result might not be plausible. The test of plausibility (see **Figure 7**) is based on the comparison of fatigue limit of virgin specimens modified by the predicted residual (mean) stress in the bulk of the nitride specimens (dashed-and-dot line) with the bending stress along the whole specimen radius, applied at the fatigue limit of nitrided specimens (full line). The difference between the applied bending stress and the fatigue limit as a function of the depth is plotted by the dotted line in **Figure 7**.

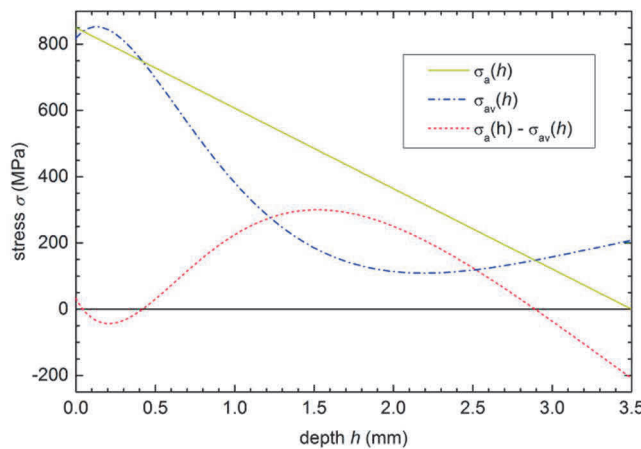


Figure 7 Comparison of fatigue limit of virgin specimens modified by the predicted residual (mean) stress in the bulk of the nitride specimens ($\sigma_{av}(h)$) with the bending stress along the whole specimen radius, applied at the fatigue limit of nitrided specimens ($\sigma_{av}(h)$). The difference between the applied bending stress and the modified fatigue limit of virgin specimens ($\sigma_a(h) - \sigma_{av}(h)$) is also plotted.

The highest difference corresponds to the depth of 1.6 mm, where the centres of fish eyes should have been preferentially found on the fracture surfaces of nitrided specimens already at the fatigue limit. This depth corresponds to the location of the high tensile residual stresses well outside the nitrided layer. However, no fish-eyes were found in this location even in specimens fractured under applied bending stresses higher than the fatigue limit. Such an overestimation of the magnitude of residual stresses is caused by the fact that the S-N curve for virgin specimens lies too much below that for the nitrided specimens. This is a consequence of large surface intrusions induced by turning which extremely reduce the fatigue resistance of virgin specimens when compared to that of the bulk of nitrided specimens. Thus, the turning lies beyond the acceptable range of the surface machining.

5. CONCLUSIONS

The original method uses the difference between the bulk S-N curve surface hardened specimens and that for the virgin specimens as a measure of residual stress levels in the depths corresponding to initiation sites of fish-eye cracks. This method is relevant only when the surface of virgin specimens is sufficiently smooth to avoid the initiation of fatigue cracks from large surface defects (artificial intrusions) made by machining. Identification of the range of its applicability is the aim of recently started systematic investigations. The research started with samples of extremely rough surfaces finished by turning which left circumferential scratches on the surface even visible to the naked eye. The analysis yielded maximum compressive stresses of about 700 MPa at the hardened surface but too high maximum tensile stresses of 500 MPa in the specimen bulk. The test of the plausibility of the result, based on the identification of the most probable depth of finding fish-eye centres, predicted depths significantly higher than the real ones. This can be attributed to the large surface intrusions induced by turning which extremely reduce the fatigue resistance of virgin specimens when compared to that of the bulk of nitrided specimens. Thus, the turning lies beyond the acceptable range of surface machining.

ACKNOWLEDGEMENTS

This research was supported by the Slovak Research and development Agency in the frame of the grant APVV-15-0710, by the Slovak Grant Agency VEGA - number of the project 1/0432/17 and by the Specific University research of Brno University of Technology in the frame of the project FSI-S-17-4504.

REFERENCES:

- [1] POKLUDA, J., KIANICOVÁ, M. Damage and Performance Assessment of Protective Coatings on Turbine Blades. *In Gas Turbines*, Ed. Gurrappa I., Rijeka: SCIYO, 2010, pp. 283-306.
- [2] NOYAN, I.C., COHEN, J.B. *Residual stress*. New York: Springer-Verlag Inc., 1986.
- [3] SIRIN, S.Y., SIRIN, K., KALUC, E. Effect of the ion nitriding surface hardening process of fatigue behaviour of AISI 4340 steel, *Materials Characterisation*, 2008, vol. 59, pp. 351-358.
- [4] SURESH, S. *Fatigue of Materials*. Cambridge: University Press, 1998.
- [5] SLÁMEČKA, K., POKLUDA, J., KIANICOVÁ, M., MAJOR, Š. DVOŘÁK, I.: Quantitative Fractography of Fish-Eye Crack Formation under Bending-Torsion Fatigue. *International Journal of Fatigue*, 2010, vol. 32, pp. 921-928.
- [6] MARINES-GARCIA, I., PARIS, P. C., TADA, H., BATHIAS, C. Fatigue crack growth from small to long cracks in VHCF with surface initiations. *International Journal of Fatigue*, 2007, vol. 29, pp. 2072-2078.
- [7] MURAKAMI, Y. *Metal Fatigue: Effects of Small Defects and Nonmetallic Inclusions*. Oxford: Elsevier, 2002.